Spectral Signatures of Transient Heating in the Solar Corona

Taroyan, Youra; Burrows, Keiran

Published in:
Journal of Physics: Conference Series

DOI:
10.1088/1742-6596/440/1/012010

Publication date:
2013

Citation for published version (APA):
Taroyan, Y., & Burrows, K. (2013). Spectral Signatures of Transient Heating in the Solar Corona. *Journal of Physics: Conference Series*, *440*(Conference 1), [012010]. https://doi.org/10.1088/1742-6596/440/1/012010

Spectral Signatures of Transient Heating in the Solar Corona

2013 J. Phys.: Conf. Ser. 440 012010

(http://iopscience.iop.org/1742-6596/440/1/012010)

Journal of Physics: Conference Series **440** (2013) 012010 doi:10.1088/1742-6596/440/1/012010

Spectral Signatures of Transient Heating in the Solar Corona

Youra Taroyan and Keiran Burrows

Institute of Mathematics and Physics, Aberystwyth University, Aberystwyth, SY23 3BZ, UK

E-mail: yot@aber.ac.uk

Abstract. Hinode/EIS observations of an active region are presented. Intensity and Doppler velocity maps for different emission lines are constructed. Consistent with previous results, the Doppler velocities near the footpoints of coronal loops appear to be blue shifted for emission lines with temperatures above 1 MK. The gradual transition from blue shifts at temperatures above 1 MK to red shifts at temperatures below 1 MK is addressed through numerical modeling of loop dynamics. The simulation results are converted into synthetic EIS observations and compared with the actual measurements. Persistent blue shifts, blue wing enhancements, and red shifts observed in EUV lines are interpreted as a signature of repetitive heating occurring near the loop footpoints on a time scale of several minutes.

Hinode/EIS observations have revealed persistent blue-shifts in active regions (Hara et al. 2008; Doschek et al. 2008; Tian et al. 2011). The blue-shifts are usually seen near the footpoints of coronal magnetic loops and may last for days or weeks. Blue shifts of up to 20 km s^{-1} were derived using single Gaussian fits to approximate coronal emission line profiles. Significant deviations from a single Gaussian profile were found in the blue wing of the line profiles. These deviations were studied using multiple Gaussian fitting (Peter 2010) and the blue-red asymmetry technique (Tian et al. 2011). Depending on the applied method, blue shifts between 30 and 100 km s^{-1} were derived.

A study carried out by Patsourakos & Klimchuk (2006) treats a single loop as a bundle of thin threads which are continually heated by nanoflares. The nanoflares result in upflows and broad line widths in the corona. The model has been critically discussed by Peter (2010). Hansteen et al. (2010) studied heating caused by the braiding of the photospheric magnetic field which produces a bi-directional flow of material from the heating site: there are downflows in transition region lines and slight upflows of a few km s^{-1} in low coronal lines. Murray et al. (2010) proposed an outflow scenario based on active region expansion, whereas Bradshaw et al. (2011) interpreted the observations by Hara et al. (2008) in terms of interchange reconnection at the boundaries between open and closed magnetic field regions.

Recently Warren et al. (2011), McIntosh et al. (2012) have detected upflows accompanied by enhanced blue wings in high temperature lines and downflows in low temperature lines. SDO/AIA observations by Kamio et al. (2011) have revealed high speed hot upflows and cool downflows in active regions. A link between short lived ($\sim$ 100 s) type II spicules and upflows in coronal loops was suggested by De Pontieu et al. (2011).

The present Letter will address the nature of the EUV Doppler shifts through a combination of data analysis and numerical forward modeling.

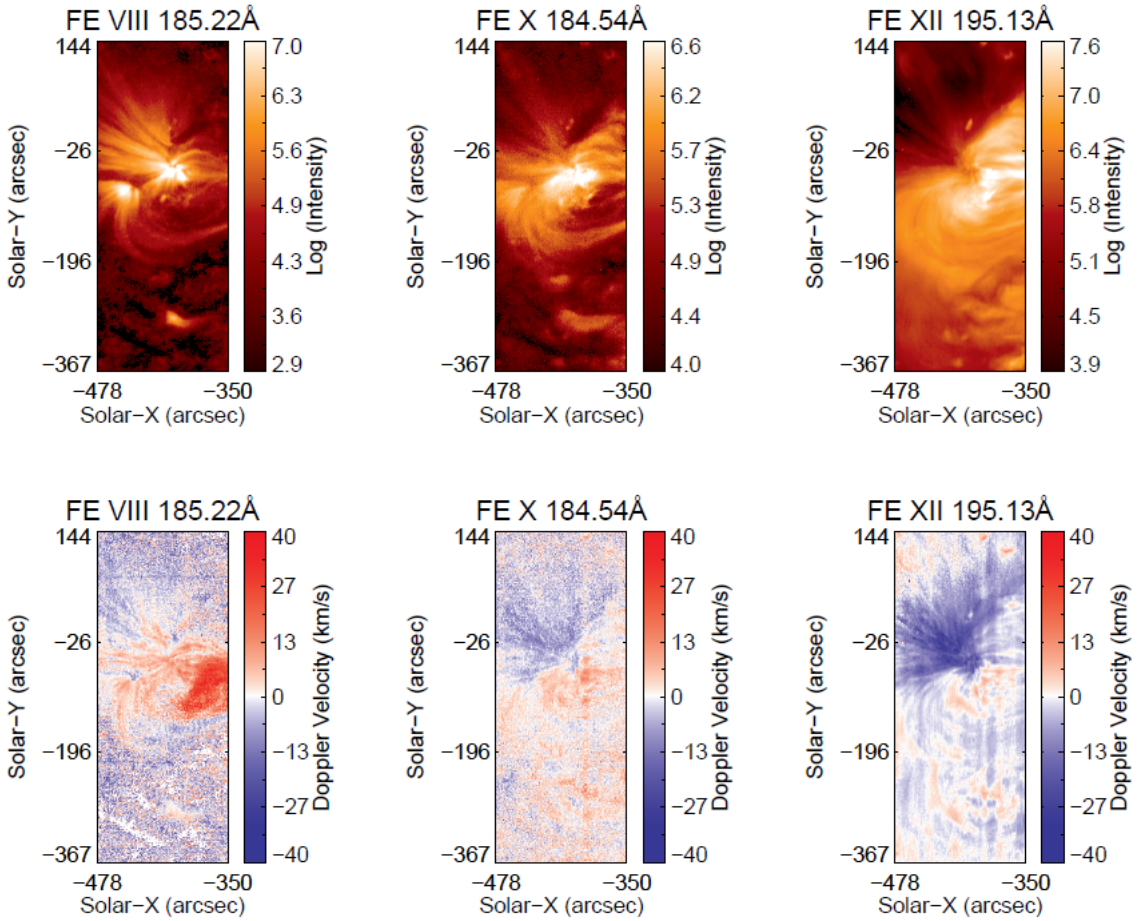

Figure 1. Intensity and Doppler velocity maps of an active region in three selected lines: Fe VIII 185 Å, Fe X 184.5 Å and Fe XII 195 Å.

1. Observations

The EUV imaging-spectrometer (EIS) aboard Hinode has two CCDs covering the wavelength ranges $171-212$ Å and $245-291$ Å. EIS has both narrow ($1''$ and $2''$ wide) slits, and wider ($40''$ and $266''$) imaging slots, all with up to $512''$ in the solar Y direction. Spectroscopic observations can be carried out either in sit-and-stare or in scanning modes. Further details of Hinode/EIS characteristics are given by Culhane et al. (2007), Kosugi et al. (2007).

For this study, we concentrated on an active region visible on 20th February 2007. Hinode/EIS observations of the active region were carried out using the $1''$ wide slit in scanning mode. Spectral data for a number of wavelengths were produced. The data have been studied by Warren et al. (2011), Martinez-Sykora et al. (2011).

In the following analysis, we select the Fe VIII 185.21 Å, Fe X 184.54 Å and Fe XII 195.12 Å spectral lines with formation temperatures of $\log T \approx 5.8$, 6.0 and 6.2. EIS level zero data files are processed with the eis_prep software, using the default options. The eis_wave_corr procedure and the level one data are used to calculate the wavelength corrections for each spectral line. We fit a single Gaussian profile to each line spectrum, using the eis_auto_fit software. The reference wavelength of each line profile has been updated to match the rest wavelength found in a laboratory, and is taken from Brown et al. (2008). EIS Doppler velocities need calibrating against a reference wavelength, where the quiet Sun velocity averages to zero. For this work the Fe VIII 185 Å line is chosen as a reference. The other lines are calculated

relative to the final wavelength of this line. Doppler velocity measurements require the slit tilt and thermal drift of the instrument to be calculated accurately. This is achieved using the eis_update_fitdata procedure, which updates these parameters, based on the fitted line profile and the first approximations from eis_wave_corr. Finally we output intensity and Doppler velocity maps for the spectral lines.

The intensity maps in Figure 1 show loops that become bright in the higher temperature line of Fe XII 195 Å. The loops are connected to the footpoints which can be seen near the center of the intensity image in Fe VIII 185 Å. The Doppler velocity maps in the lower panel reveal the presence of blue shifts in Fe XII near the footpoints. The blue shifts fade out in Fe X and turn into red shifts in the lower temperature Fe VIII line. The blue shifts at high temperatures are a persistent feature of EIS observations and may last for prolonged periods of time (e.g., Hara et al. 2008). The footpoints areas of the cool loops in Fe VIII are red shifted whereas the footpoint areas of the hot loops in Fe XII are blue shifted. The velocities for the intermediate Fe X line are close to zero. This gradual transition from red to blue will be addressed in the forthcoming analysis which is based on numerical forward modeling.

In addition to loop like structures, Figure 1 shows fan like structures at the top left corner of the image. These structures mainly appear bright in the lower temperature line of Fe VIII 185 Å. The question whether the blue shifts seen in the Fe XII velocity map are related to the fan like structures has been addressed by Warren et al. (2011).

2. Numerical Forward Modeling

In order to explain the features seen in Figure 2, in particular, the gradual transition from red in Fe VIII to blue in Fe XII near the loop footpoints, we carry out numerical forward modeling. A single loop with a typical length of 40 Mm is initially in a cooling state due to the combined action of thermal conduction and radiation. The loop is gravitationally stratified and remains in the vertical plain. Cooling leads to downflows along the loop legs. Only longitudinal motions are considered. Motions in other directions are ignored. This is a valid approximation as long as the ratio of the thermal pressure to magnetic pressure is small. The initial peak temperature at the apex is about 0.6 MK and the dense chromospheric footpoints are kept at a constant temperature of 20 000 K. The governing equations of continuity, momentum and energy are integrated numerically to investigate the loop response to transient heating. The one dimensional treatment and the adaptive mesh refinement technique allows us to accurately model the dynamics in the steep transition region and the emission in EUV lines. The details of the HYDRAD code used in our modeling are described by Bradshaw & Mason (2003).

A phenomenological heating term is included in the energy equation. The heating is located 3 Mm inside the chromospheric boundary and it has an exponential scale height of 4 Mm. Localizing the heating near the footpoints has the effect of driving strong upflows. For simplicity, a symmetric profile about the apex is chosen. The heating occurs on a time scale of a few minutes. It smoothly increases from $t = 0$ s, reaches its peak rate at $t = 150$ s and vanishes at $t = 300$ s. The subsequent dynamics is determined by thermal conduction and radiation. The amount of energy input is proportional to the cross sectional area of the loop. For a cross sectional diameter of 1 Mm the total energy input near each footpoint is about 10^{26} erg. The selected heating parameters are best suited for reproducing the observed temporal evolution.

Figure 2 displays the evolution of the loop. The vertical axes denote distance along the loop. Temperature starts to rise after heating catches up with losses. The loop reaches a peak temperature of 3 MK at about $t = 200$ s. The second panel of Figure 2 shows strong upflows along both legs during the heating stage which leads to high temperatures. During this stage a maximum upflow speed of 110 km s^{-1} is reached. The subsequent evolution of the loop is dominated by downflows as the loop cools to lower temperatures. The initial state is approximately restored at the end of the simulation.

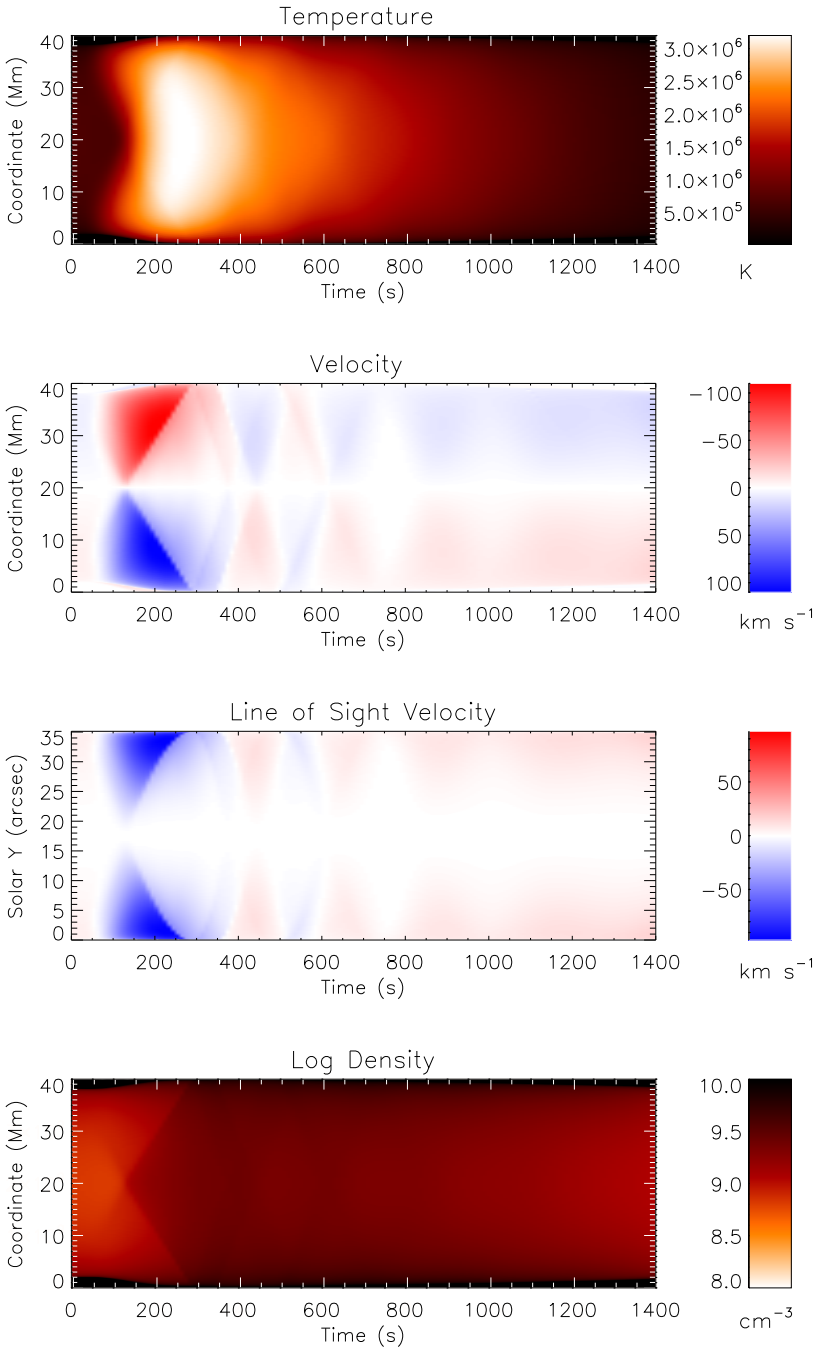

Figure 2. The evolution of the loop during the first 1400 s. Temperature, velocity along the loop and density are plotted as functions of time and loop coordinate. The third panel displays the line of sight velocity.

The velocities projected onto the line of sight are shown in the third panel of Figure 2. For simplicity, it is assumed that the loop is located in the center of the solar disc. Note the shift of the peak velocities towards the footpoints due to the semicircular geometry of the loop.

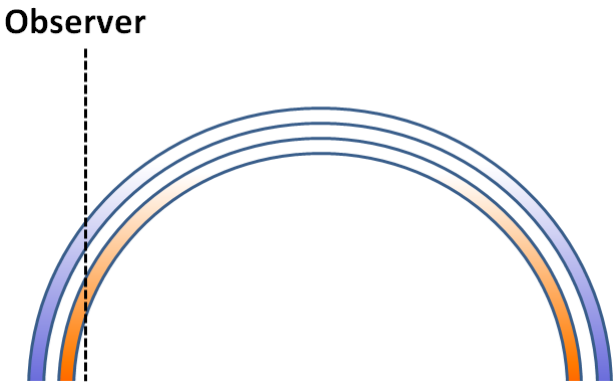

Figure 3. Three loops intersecting with the line of sight. The colours indicate different states: upflows (blue), downflows, (red), no flows (white).

Downflows correspond to positive red-shifts, and upflows correspond to negative blue shifts. The heating pulse leads to blue shifts of up to 97 km s^{-1}. The bottom panel of Figure 2 displays the evolution of density: heating and upflows are followed by enhanced density whereas cooling and downflows reduce the amount of material in the loop.

3. Discussion

Figure 2 suggests that the evolution of the loop proceeds in three main stages: there are blue shifts near the footpoints at high temperatures and red shifts at low temperatures. The velocities are small at intermediate temperatures when there is a transition from heating to cooling or vice-versa. However, the blue shifts observed in high temperature lines are usually quite persistent and last much longer than the flows in our simulations (Hara et al. 2008). Another important difference is that Figure 1 shows an entire active region, whereas our simulations are carried out for a single loop. It is therefore not possible to directly reproduce the observed behavior from the simulations.

According to the observations presented in Figure 1, there might be several loops along the line of sight. In general, the loops have different densities, temperatures, lengths, widths, inclinations, etc, and are in different stages of evolution as shown in Figure 3. All these loops converege at the footpoints where the blue shifts are mainly seen. In the absence of detailed knowledge of the involved parameters, we assume that there are four loops along the line of sight which are almost identical if their length is large compared to the cross sectional radius. Each loop follows the cycle shown in Figure 2 which is repeated upon completion and there is a lag time of 250 s between the loops.

The simulation results are converted into synthetic spectral observations using the EIS response function. The full details of this procedure are described by Taroyan et al. (2006). The emission from the three loops shown in Figure 3 is integrated along a segment near the footpoints. The length of the segment corresponds to a $1''$ EIS slit. The instrumental width of the EIS instrument is added to the thermal width of the line profile.

Figure 4 shows synthetic line profiles constructed for Fe VIII, Fe X Fe XII at different moments of time. Each plotted curve represents a superposition of three spectral line profiles representing different loops.

A comparison between the observations and the synthesized spectral line profiles reveals similarities. In both cases, the low temperature Fe VIII lines are predominantly red shifted. These are cooling loops dominated by downflows. The Fe X Doppler shifts are small. This type of emission mainly corresponds to loops at intermediate temperatures that are in a transition

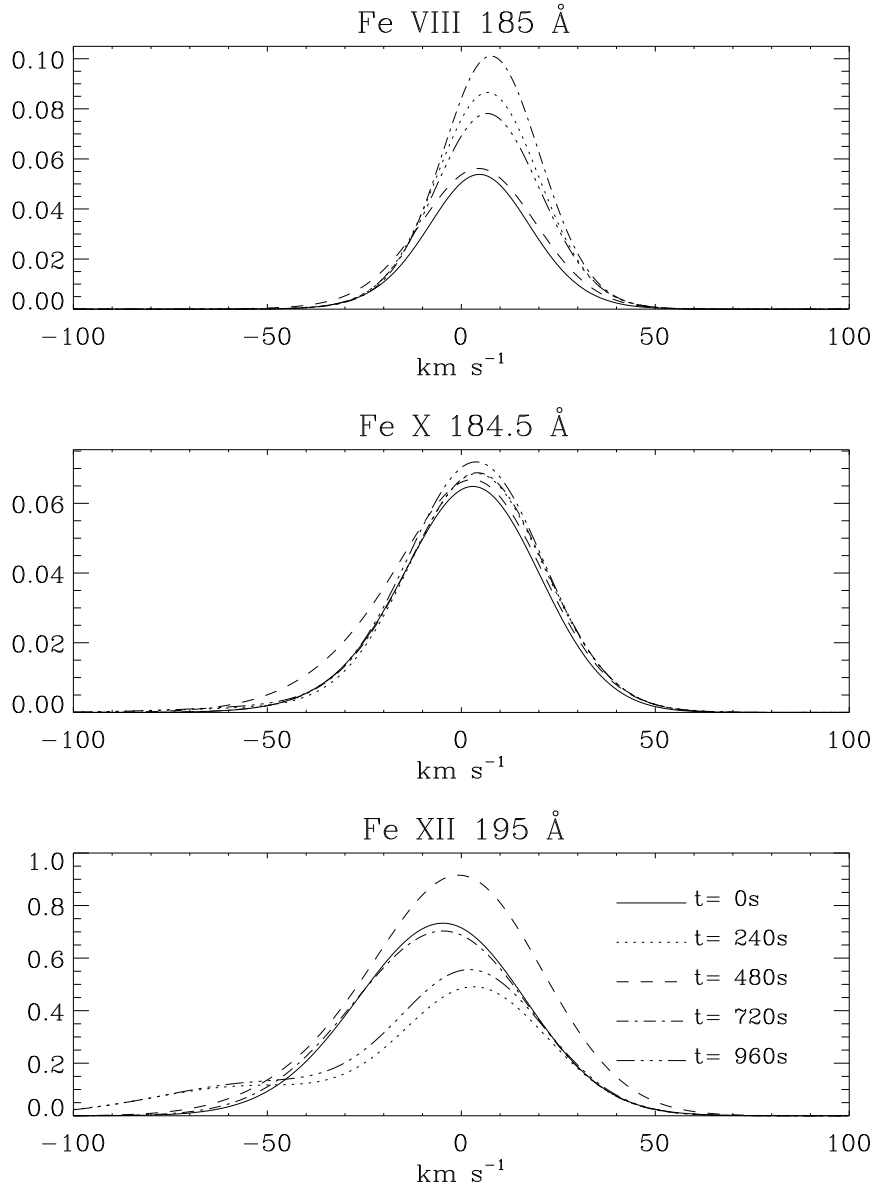

Figure 4. Synthesized spectral line profiles at different moments of time. Each curve represents a superposition of four different line profiles which correspond to identical loops in different states.

from heating to cooling or vice-versa. Blue shifts and enhanced blue wings appear with increasing temperature in Fe XII and Fe XV. The enhanced blue wings representing high speed flows become most prominent in the high temperature Fe XV line. These types of line profiles are associated with loops that are in the heating stage.

The relatively higher intensities in Fe VIII and Fe X can be explained by the presence of underlying cool structures that are not taken into account by the model. Despite the mentioned differences that are mainly due to the simplicity of our model, the agreement with the observations is encouraging.

A comparison of spectral observations with forward modeling supports the idea of heating

on a time scale of a few minutes. Blue shifts and blue wing enhancements are associated with heating, whereas the red shifts are a signature of cooling. No such clear association exists when the heating time scale is significantly reduced. We have performed a sample simulation of heating with a similar total energy input but with a duration of 60 s: strong red shifts appear during the heating stage and blue shifts appear during the cooling stage as the rapid pressure pulse bounces back and forth along the loop. It is therefore no longer possible to reproduce the observations shown in Figures 1. A significant increase in the total heat input leads to higher maximum temperatures but results in red shifts at temperatures above 1 MK. We have therefore found important constraints on models of loop heating.

Below we explain the absence of significant net shifts in the case of rapid heating. The initial heating event drives evaporation from the chromosphere which lasts for a short period of time. The emission is expected to peak during the cooling phase when the densities are high. However, these brief upflows propagate away from the footpoint segment of the loop by the time it cools to the Fe XII passband and no significant upflows are seen. Subsequently the pulse is propagating and bouncing back and forth along the loop as the loop cools to Fe X and Fe VIII passbands. This may result in blue, red or no shifts. Therefore a superposition of rapidly heated loops leads to a situation whereby no significant net flows are detected. Therefore, no significant net flows will be detected if the heating time is short compared with the pulse travel time. The travel time is roughly determined as the ratio of the loop length and the sound speed. When the loops are longer than about 20 Mm, the reflection effects become small and therefore blue shifts and red shifts are seen at high and low temperatures, respectively.

4. Conclusions

The coexistence of blue shifts in coronal lines and red shifts in transition region lines has been known for many years. These persistent features have mainly been interpreted as a manifestation of a bi-directional flow of material from the reconnection site or nanoflares (Teriaca et al. 1999; Hansteen et al. 2010; Patsourakos & Klimchuk 2006). Hinode/EIS observations have revealed new features near the footpoints of active region loops. Figures 1 and 4 show red shifts at low temperatures (Fe VIII line), blue shifts and enhanced blue wings at high temperatures (Fe XII and Fe XV lines). All these features are reproduced from numerical simulations of transient loop heating if the convergence of several loops at the footpoints is taken into account. The heating occurs on a time scale of a few minutes. The nature of the heating process remains unknown. However, the obtained results provide important constraints on models of loop heating.

[1] Bradshaw S. J. & Mason H. E., 2003, A&A, 407, 1127
[2] Bradshaw, S. J., Aulanier, G., Del Zanna, G., 2011, ApJ, 743, 66
[3] Brown, C. M., Feldman, U., Seely, J. F., et al., 2008, ApJS, 176, 511
[4] Culhane, J. L., et al., 2007 Sol. Phys., 243, 19
[5] De Pontieu, B., McIntosh, S. W., Carlsson, M., et al., 2011, Science, 331, 55
[6] Doschek, G. A., Warren, H. P., Mariska, J. T., et al., 2008, ApJ, 686, 1362
[7] Hansteen, V. H., Hara, H., De Pontieu, B., et al., 2010, ApJ, 718, 1070
[8] Hara, H., Watanabe, T., Harra, L. K., et al., 2008, ApJ, 678, L67
[9] Kamio, S., Peter, H., Curdt, W., et al., 2011, A&A, 532, A96
[10] Kosugi, T., et al., 2007, Sol. Phys., 243, 3
[11] Martinez-Sykora, J., De Pontieu, B., Hansteen, V., et al. 2011, ApJ, 732, 84
[12] McIntosh, S. W., Tian, H., Sechler, M., et al., 2012, ApJ, 749, 60
[13] Murray, M. J., Baker, D., van Driel-Gesztelyi, L., et al. 2010, Sol. Phys., 261, 253
[14] Patsourakos, S. Klimchuk, J. A., 2006, ApJ, 647, 1452
[15] Peter, H., 2010, A&A, 521, A51

[16] Peter, H. & Judge, P. H., 1999, ApJ, 52
[17] Taroyan, Y., Bradshaw, S. J., & Doyle, J. G., 2006, A&A, 446, 315
[18] Teriaca, L., Doyle, J. G., Erdlyi, R. et al., 1999, A&A, 352, L99
[19] Tian, H., McIntosh, S. W., De Pontieu, B., et al., 2011, ApJ, 738, 18
[20] Warren, H. P., Ugarte-Urra, I., Young, P. R., et al., 2011, ApJ, 727, 58